J. Plasma Physics (2006), *vol.* 72, *part* 2, *pp.* 229–239.
doi:10.1017/S0022377805003910 First published online 25 November 2005 Printed in the United Kingdom

On the dynamics of a non-equilibrium Cu plasma produced by an excimer laser interaction with a solid

D. DORIA, A. LORUSSO, F. BELLONI and V. NASSISI

Applied Electronics Laboratory, Physics Department of the University of Lecce, INFN Lecce, CP 193, 73100 Lecce-I, Italy
(vincenzo.nassisi@le.infn.it)

(Received 25 November 2004 and accepted 30 January 2005)

Abstract. We report here on the expansion dynamics of a non-equilibrium plasma produced by an excimer laser interaction with a Cu solid target. Its characteristics were investigated in the fast and slow time regime by two Faraday cups of different diameter. The larger cup had an 8 cm diameter collector and was fixed along a drift tube at a distance of 20 cm from the plasma source; the smaller cup had a 3.3 cm diameter collector and was fixed transversally to the target at a distance of about 6 cm. During the experiments the target support signal was also recorded. The laser beam was focused onto the target and the spot dimensions were analysed by scanning it on the lens focal plane. An average power density on the target of 0.3 GW cm^{-2} was achieved with a 15 cm focal length lens. Using signals from the Faraday cups we obtained information on the overall plasma evolution in the slow and fast time regimes. Fitting the plasma current waveform by a 'shifted' Maxwell–Boltzmann distribution, a Knudsen-layer temperature of 5.3×10^5 K ($\sim$50 eV) and a drift velocity of 5300 m s^{-1} resulted. The system efficiency in ablation yield and ion production was 0.235 μg pulse^{-1} and 5×10^{13} ion pulse^{-1}, respectively.

1. Introduction

Since the 1980s, in coincidence with the proliferation of powerful laser sources, the pulsed laser ablation (PLA) of solid targets has become of wide interest for its manifold applications and the attractive processes involved. This ablation method is being investigated for application in the generation of multiple-charge ions [1, 2] and the deposition of thin films of very complex materials [3, 4]. In fact, the high plasma temperature involved in these experiments [5] is very promising for creating ions in a high charge state, favoring the development of ion beams able to feed large ion accelerators. These devices, devoted to the production of laser-induced ions, are called laser ion sources (LISs).

Owing to the high laser fluence necessary to obtain ablation, the target heats up to its boiling temperature. The vapors produced are subsequently ionized and heated via inverse bremsstrahlung, reaching a plasma temperature much higher than that of the target. The target temperature is dependent on the laser beam parameters and the chemical–physical properties of the target material.

The extreme speeds of the processes involved do not allow one to obtain direct measurements of the plasma temperature. Even with this drawback, its value can be deduced by analyzing the particle velocity distribution. In fact, fits by a modified Maxwell–Boltzmann function are usually employed [6].

During the initial phase, the plasma formation results in a high concentration of electrons, ions, atoms, molecules and clusters. This characteristic implicates a low Debye length ($\lesssim$1 mm), the value of which becomes comparable to the evolving plasma dimensions. This condition favors the escape of the most energetic particles and, after a few nanoseconds, the plasma undergoes an adiabatic expansion [7]. During this phase even the internal electric field strength and plasma geometry vary, and some of ions can be accelerated at high velocity [8], reaching energies of some keV [9].

A task in thin-film deposition by PLA is to forecast the film profile in order to improve its quality. For this reason studies have been carried out thinking of the plasma only as a neutral gas [10]. Considering the plasma as a plume of neutral particles, one excludes the influence of the charged components on the film quality. Therefore, even for these reasons, it is necessary to know the angular distributions of both charged and neutral plasma particles.

To characterize the plasma expansion, in this paper we study the behavior of a plasma created by the interaction of an ultraviolet (UV) laser with a Cu solid target. The most meaningful measurements were the efficiency of the system in terms of the ablation yield, the longitudinal temperature of the plasma and the ion production.

2. Theory

The laser ablation process employs a very large laser fluence (tens of J cm^{-2}). It instantly turns the target to liquid, and to the gaseous phase at the thermodynamic critical temperature, T_{tc}. Therefore in these experiments, due to the thermally activated target, many processes must be considered [11] in order to explain the experimental results. During the formation of the plasma, electrons escape and the plasma expands perpendicularly to the target surface (x-direction). The particle initial velocity along the x-axis is $v_x \geqslant 0$. For low particle density values, when the emission is collisionless, the escaping velocity v_x remains approximately the same during the expansion. In contrast, for high density values, it has been demonstrated [12] that the particles, emitted with velocity $v_x \geqslant 0$, undergo sufficient collisions to modify their initial velocity, reaching negative values, namely $-\infty < v_x < +\infty$. This phenomenon occurs near the target surface, where the particles collide, and this region is called the Knudsen layer (KL). In the transversal z- and y-directions, the velocity ranges over $-\infty < v_z, v_y < +\infty$, but the average values $\langle v_z \rangle$ and $\langle v_y \rangle$ are zero. By these considerations, the initial distribution function of the particles on velocities is Maxwellian:

$$f_{\mathrm{target}} \propto \exp\left[-\frac{2E + mv_x^2}{2kT_{\mathrm{t}}}\right] \exp\left[-m\frac{v_y^2 + v_z^2}{2kT_{\mathrm{t}}}\right], \tag{1}$$

where the average velocity in the x-direction is estimated to be

$$\langle v_x \rangle = \sqrt{\frac{2kT_{\mathrm{t}}}{\pi m}}. \tag{2}$$

https://doi.org/10.1017/S0022377805003910 Published online by Cambridge University Press

In (1) and (2), T_t is the target temperature, k is the Boltzmann constant and E is the total internal energy of the particle. Since $\langle v_x \rangle$ is different from zero, it can be regarded as a velocity of the center of mass (COM). Then, taking into account the collisions in the KL, the longitudinal temperature of the plasma decreases. Now, beyond the KL region, we have the KL distribution function, with $-\infty < v_x, v_y, v_z < +\infty$, of the form

$$f_{\mathrm{KL}}(v_x, v_y, v_z, E) \propto \exp\left[-\frac{2E + m(v_x - v_d)^2}{2kT_{\mathrm{KL}}}\right] \exp\left[-m\frac{v_y^2 + v_z^2}{2kT_{\mathrm{KL}}}\right], \tag{3}$$

where v_d represents the COM velocity and T_{KL} is the KL temperature.

The temporal behavior of the neutral component cannot be investigated by electromagnetic probes, while the temporal behavior of the charged particles can be easily studied using time-of-flight (TOF) measurements. The signals can be obtained using polarized Faraday cups.

So, to evaluate the ion current collected in a solid angle centered on the x-axis, (3) has to be integrated on v_y, v_z and E. Applying polar coordinates we obtain

$$f_{\mathrm{KL}}(v_x)\, dv_x \propto \exp\left[-\frac{m}{2kT_{\mathrm{KL}}}(v_x - v_d)^2\right] g(v_x)\, dv_x \tag{4}$$

with

$$g(v_x) \propto \int_0^{(R/x)v_x} v_n \exp\left[-m\frac{v_n^2}{2kT_{\mathrm{KL}}}\right] dv_n$$

$$= \frac{kT_{\mathrm{KL}}}{m}\left\{1 - \exp\left[-\frac{m}{2kT_{\mathrm{KL}}}\left(\frac{R}{x}\right)^2 v_x^2\right]\right\},$$

where $v_n = \sqrt{v_y^2 + v_z^2}$ is the transversal velocity and R is the collector radius.

Under our experimental conditions, the plasma is approximately generated from a small spot on the target and, as a consequence, at a distance x all the particles with the same v_x velocity arrive after a time t. Then, substituting x/t for v_x and $x\, dt/t^2$ to dv_x in (4), the ion current $I(t)$ recorded by the cup assumes the form:

$$I(t) \propto \frac{1}{t^2} \exp\left[-\frac{m}{2kT_{\mathrm{KL}}}\left(\frac{x}{t} - v_d\right)^2\right] g\left(\frac{x}{t}\right). \tag{5}$$

Now, fitting the experimental data by means of (5) we can determine the plasma temperature and the drift velocity.

3. Experimental apparatus and results

We utilized a home-made XeCl excimer laser ($\lambda = 308$ nm) having a 20 ns pulse duration. The energy deposited on the target was 70 mJ. The interaction chamber was made of stainless steel and its details are described in [13, 14].

In this work the experimental measurements were performed using two Faraday cups. Figure 1 shows a sketch of the chamber with the cups. One cup is large and has a collector of diameter 8 cm. The other one is small and its collector is 3.3 cm in diameter. The large one was placed along the plasma propagation direction at a distance of 20 cm from the target, while the small one was placed transverse to the target at a distance of 6 cm. Connecting them to an oscilloscope allowed the charged

https://doi.org/10.1017/S0022377805003910 Published online by Cambridge University Press

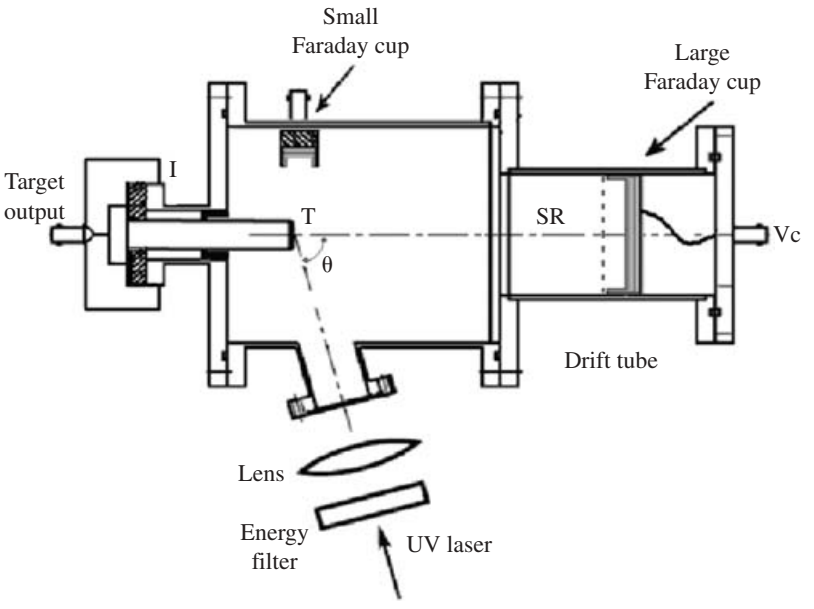

Figure 1. Experimental apparatus. The laser beam axis is tilted at $\Theta = 70^\circ$ with respect to the chamber axis.

particles ejected spontaneously from the plasma to be recorded. In order to collect the positive ions, the Faraday cups were negatively polarized. The oscilloscope was decoupled from the bias voltage by means of a 5 μF capacitor. The cup signals were terminated on a $R_{\mathrm{Load}} = 50\ \Omega$ load resistor connected to a voltage divider having an attenuation factor of 25. In such a way we were able to record the ion current.

The total cup current I_{C} is due to the ion current I_{I} plus the ion–electron secondary emission current. So, I_{I} is a fraction of I_{C} and it is governed by the following time-dependent expression:

$$I_{\mathrm{I}}(t) = I_{\mathrm{C}}(t)[1 - \sigma(t)] = \frac{V_{\mathrm{C}}(t)}{R_{\mathrm{Load}}}[1 - \sigma(t)], \tag{6}$$

where V_{C} is the cup voltage and σ is the ion–electron secondary emission function. We tested the σ value in our experiment by applying a suppression ring (SR in Fig. 1) on the cup collector [15]. We found $\sigma \approx 0$ due to the low concentration of particles having energy sufficient to extract electrons.

A 15 cm focal length lens was used to concentrate the laser beam on to the target surface. It was a disc of 99.99% pure Cu. To assess the laser spot size we analyzed it on the lens focal plane, orthogonally to the laser axis, using a joulemeter and a movable straight edge as can be seen in Fig. 2. By finely translating the straight edge with a step of 0.05 mm, we obtained the spatial integration of the spot energy. Fitting the results with the erf function we obtained the horizontal (y) and vertical (z) spot integral profile. Figure 3 shows the experimental results and the best-fit curve of the distribution along the y- and z-axes. By deriving the spot integral profiles along the y- and z-directions, we obtained the laser fluence, F, distribution:

$$F(y, z) = F_0 \exp\left[-\frac{1}{2}\left(\frac{y^2}{\sigma_y^2} + \frac{z^2}{\sigma_z^2}\right)\right], \tag{7}$$

https://doi.org/10.1017/S0022377805003910 Published online by Cambridge University Press

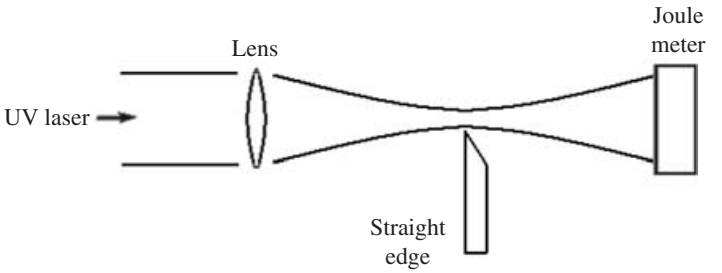

Figure 2. Spot analysis on the lens focal plane. The straight edge moves transversally to the laser–lens axis.

where the symbols have their usual meanings. Figure 4 shows the intensity distribution on the target surface along the y- and z-directions at 70 mJ laser energy. Owing to the laser axis being tilted with respect to the target surface, the intensity distribution in the y-direction is stretched with respect to the z-direction by a factor of $1/\cos 70°$. To determine the effective spot value it is necessary to know the ablation threshold fluence. For this reason we investigated the maximum energy value needed to declare the cup signals void. A value of 2.4 mJ was found. By comparison with the value of F_0 at 70 mJ pulse energy, 20 J cm^{-2}, it is evident that the corresponding threshold fluence results in a value of 0.7 J cm^{-2} (see Fig. 4). Therefore, we consider that the plasma was produced by part of the laser spot having a local fluence greater than 0.7 J cm^{-2}. So, the effective spot shape, for the laser energy utilized in this work (70 mJ) was approximately an ellipse with horizontal and vertical semi-axes of 0.76 and 0.49 mm, respectively, and an area of about 1.2 mm^2. Such a spot size gives average values of fluence and power density of 5.8 J cm^{-2} and 0.3 GW cm^{-2}, respectively, with a maximum fluence value of 20 J cm^{-2}.

Figure 5 shows the plasma signal of the large Faraday cup polarized by a bias voltage of −200 V. The large Faraday cup exhibited a positive voltage owing to its polarization. In this way we observed that the plasma reached the cup after 6 μs and its maximum intensity was recorded after 10 μs. This means that the ions have a maximum velocity of 33 km s^{-1} and a velocity at the peak of 20 km s^{-1}. The cup signal was fitted with the distribution function defined in (5), obtaining a KL longitudinal temperature of $T_{\mathrm{KL}} = 5.3 \times 10^5$ K and a flow velocity of $v_d =$ 5300 m s^{-1}. This high ion temperature value is very promising for a multiplicity of technological applications in the future. It is of the same order of magnitude as found by other authors for a pyrolytic graphite target [16].

We also estimated the duration of emission of the neutral particles, which resulted in a value of some hundreds of microseconds [14]. This result points out that particles are ejected from the target for a long time and their temperature ought to be much lower than that of the ions.

To better understand the ablation process, we compared the biased cup signal with the no-biased cup one. So, in Fig. 6 we report the same plasma signal recorded by the large Faraday cup with and without a bias voltage. The upper signal represents the output plasma current recorded with the polarized cup and displayed on a vertical scale smaller than that of Fig. 5. It reveals a small and broadened peak due to the suprathermal ions, traveling at a velocity of about 63 km s^{-1}. The lower

https://doi.org/10.1017/S0022377805003910 Published online by Cambridge University Press

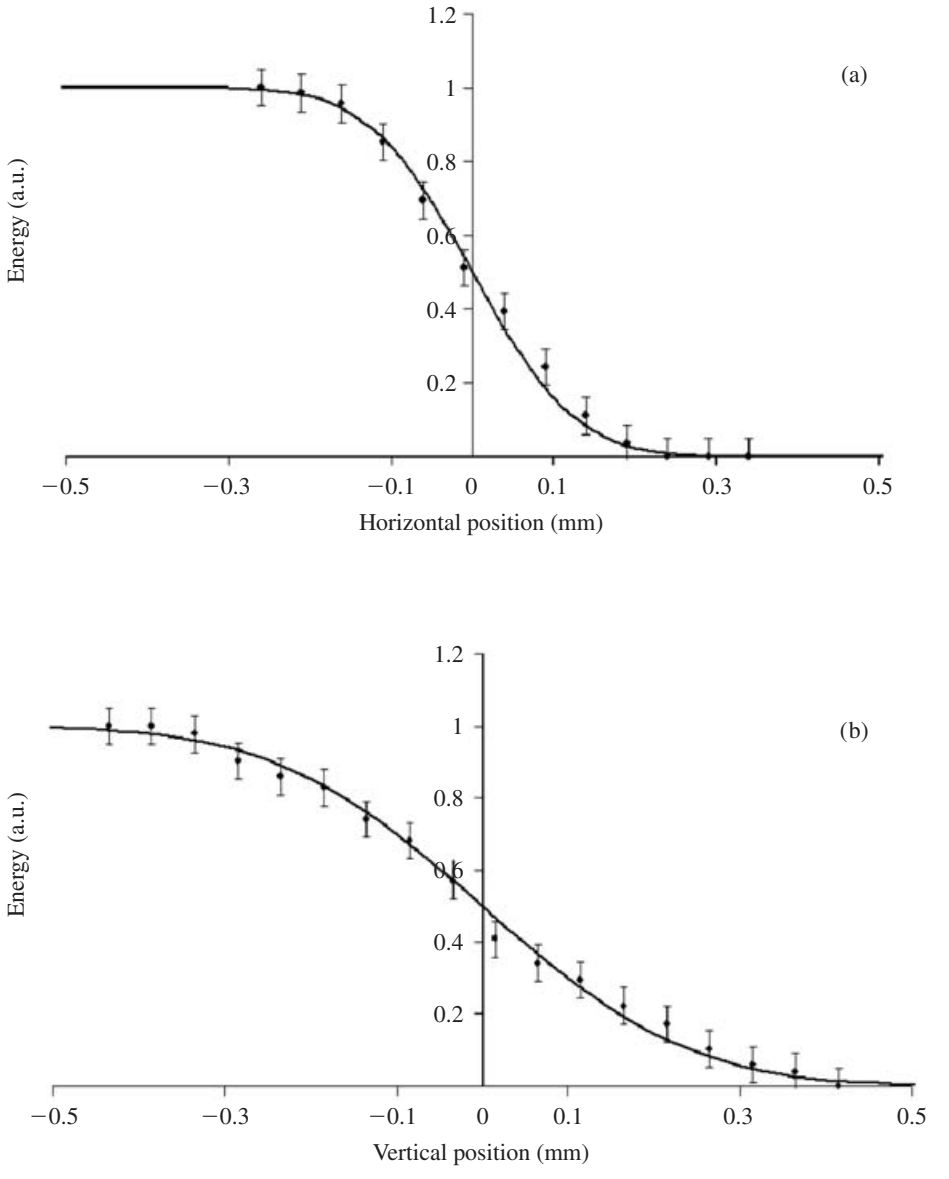

Figure 3. Laser energy integral profiles on the lens focus. (a) Data points represent the energy integral distribution along the horizontal direction (y), while the full curve represents the best-fit curve; (b) data points represent the energy integral distribution along the vertical direction (z), while the full curve represents the best-fit curve.

waveform represents the plasma signal without the cup polarization. This signal is negative as a consequence of the higher mobility of electrons in comparison with ions. At about 3 μs one can observe a small hump, which is evidently due to the suprathermal ions which, on reaching the cup, decreased the electron signal. After 5.5 μs the electron signal decreased owing to the arrival of the thermal ions.

To strengthen this hypothesis we performed similar measurements with the small cup. In Fig. 7 we report the experimental results obtained first with the small cup

https://doi.org/10.1017/S0022377805003910 Published online by Cambridge University Press

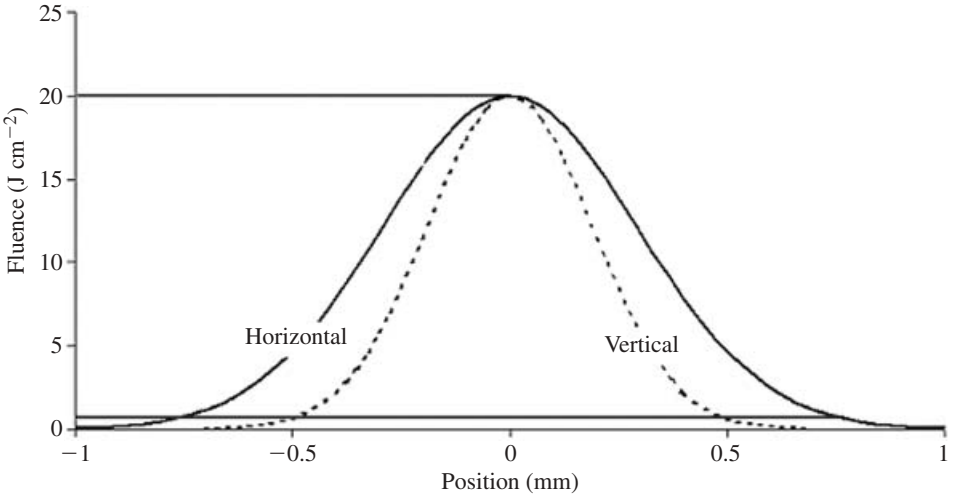

Figure 4. Fluence profiles along the horizontal direction (y-axis), stretched by a projection factor of $1/\cos 70^\circ$, and the vertical direction (z-axis).

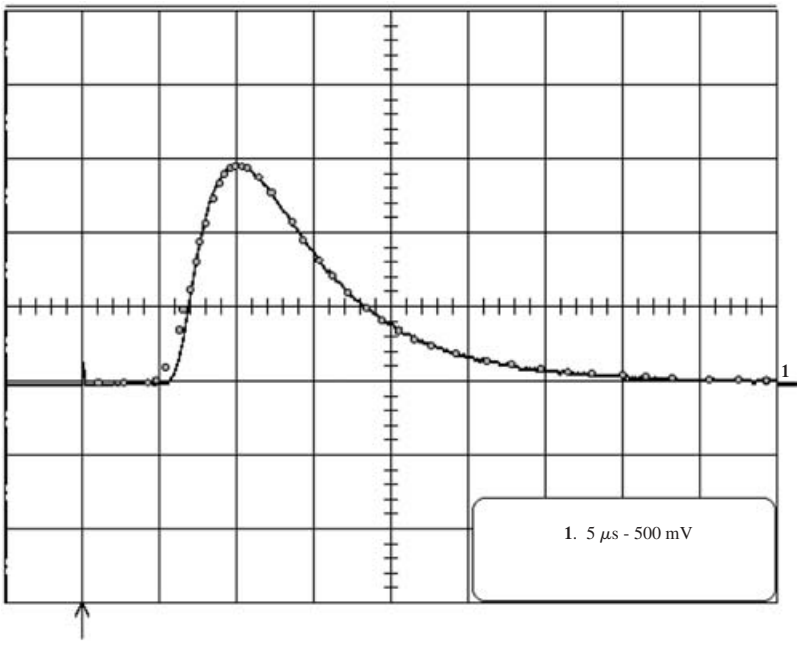

Figure 5. Ion current waveform recorded by the large Faraday cup. The cup bias voltage and the target cup distance were −200 V and 20 cm, respectively. A 25× voltage divider was used. The points represent the best-fit curve, see (5).

biased at −200 V and then without a bias voltage. Also in this way we observed a positive signal in the former case and a negative signal in the latter one. As the electrons were the cause of the negative signal, an abrupt drop was present at 1 μs corresponding to injection of the fast ions. The peak ejection velocity of the fast ions was found to be 37 km s^{-1} in the radial direction.

https://doi.org/10.1017/S0022377805003910 Published online by Cambridge University Press

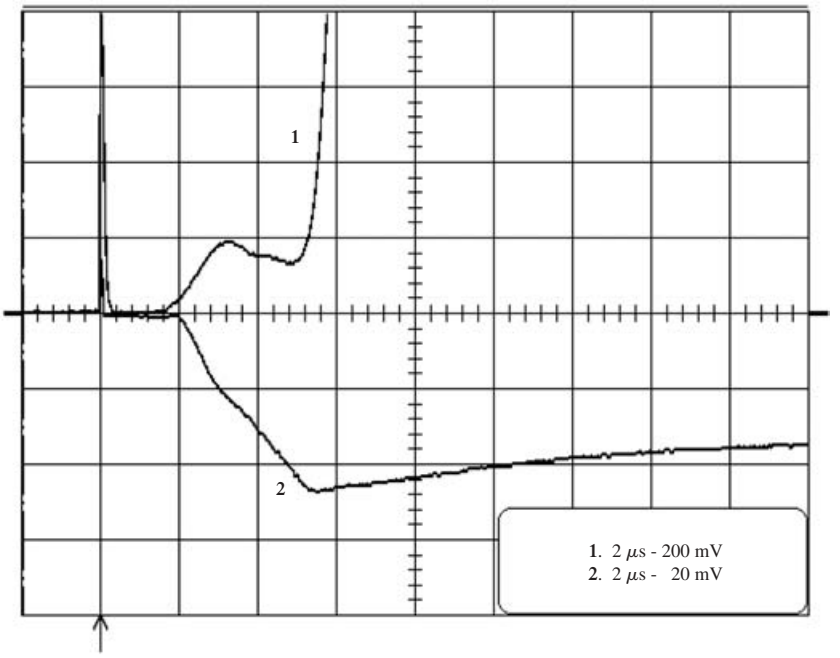

Figure 6. Large Faraday cup signals: no 1, recorded with a −200 V bias voltage, amplified to show the suprathermal ions; no 2, recorded with no bias. A 25× voltage divider was used.

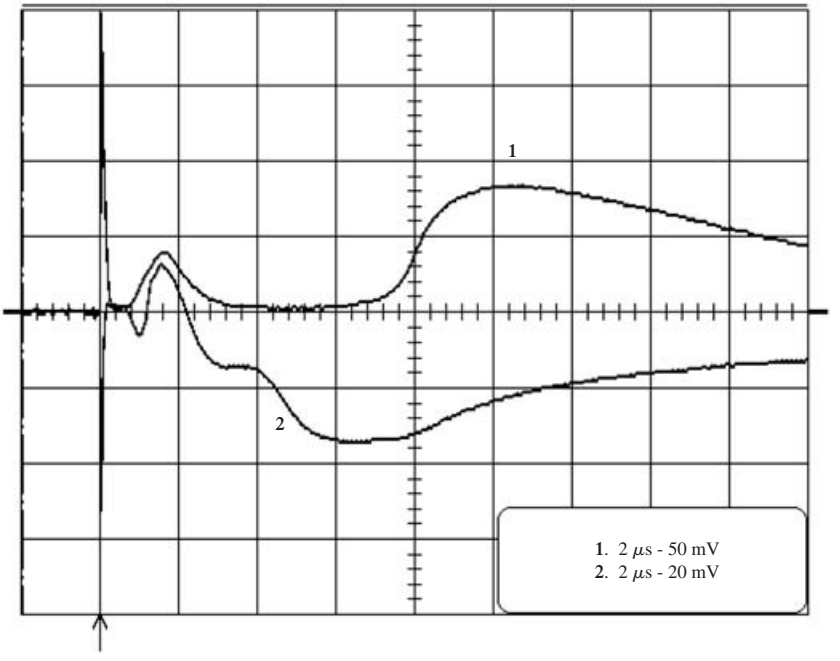

Figure 7. Small Faraday cup signals: no 1, recorded with a −200 V bias voltage; no 2, with no bias. A 25× voltage divider was used.

https://doi.org/10.1017/S0022377805003910 Published online by Cambridge University Press

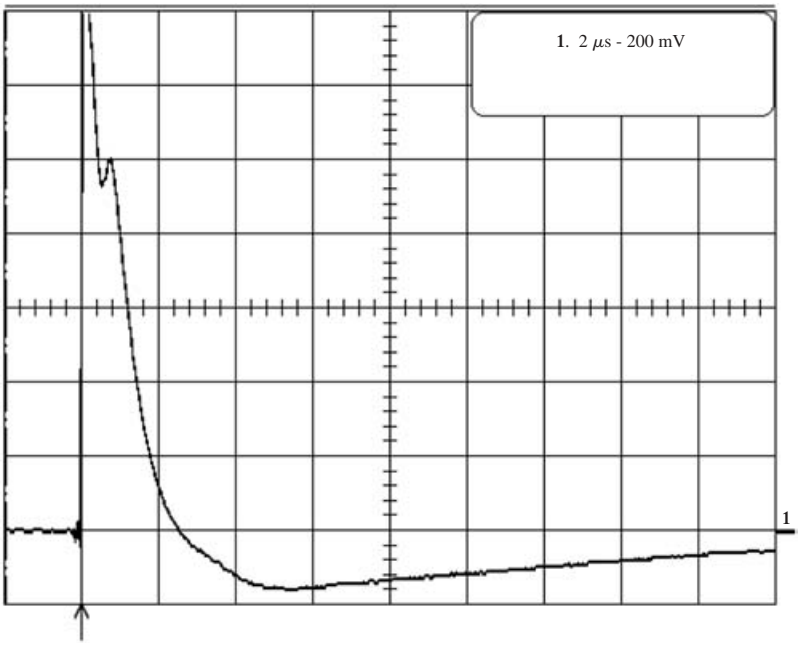

Figure 8. Target signal, recorded by connecting the target support directly to the oscilloscope.

For the thermal ions we found values of about 20 and 6 km s^{-1} for the peak velocity in the longitudinal and radial directions, respectively. This means that even a thermal plasma shows an anisotropic expansion, namely the plume is strongly forward peaked.

By a comparison with previous measurements based on the application of an electrostatic barrier [17], we conclude that the suprathermal ions had a kinetic energy of below 80 eV. Taking into account the above-mentioned velocity values, the ions could not be suprathermal Cu ions, rather they were ions from hydrogen adsorbed in the target [15].

Furthermore, we measured the target potential (Fig. 8). The target support was connected to the oscilloscope and its signal closed on 50 Ω. Its voltage was positive until 2.5 μs. In this phase the plasma is forming and this results in strong contact with the target stem. The fastest electrons leave the target, which becomes positively charged. In the meantime the plasma propagates with a velocity of about 20 km s^{-1} and its spatial dimension near the target was estimated to be about 2.8 cm [14]. For later times the target potential becomes negative. In fact, after just a few microseconds, the plasma bunch leaves the target which, as the cup does, collects electrons from the plasma bunch.

In Fig. 9 we show the onset peak of signal no 1 in Fig. 6 on a smaller time scale, 20 ns division^{-1}. Its temporal duration is greater than that of the laser pulse (signal no 2), as recorded by a fast photodiode. As the cup signal was very fast we ascribed this behavior to the soft X-rays generated from the plasma just a few nanoseconds after the laser onset time. The secondary electrons photo-extracted from the Faraday cup collector could be recorded more easily by polarizing the collector negatively. From Fig. 9 the temporal duration of the above photo-peak is

https://doi.org/10.1017/S0022377805003910 Published online by Cambridge University Press

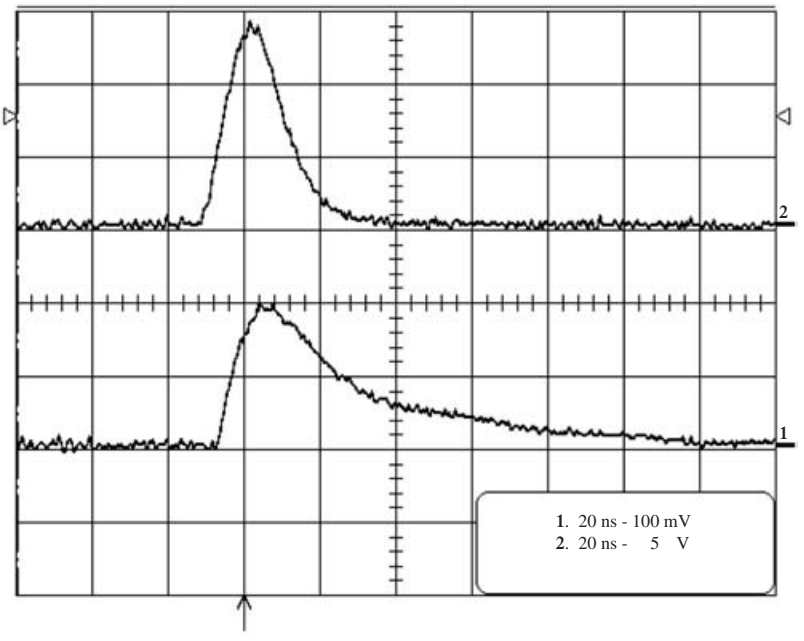

Figure 9. Comparison between the temporal evolution of the large Faraday cup photo-peak (signal no 1) and the laser pulse one (signal no 2), as recorded by a fast photodiode.

about 30 ns (FWHM) and it is reasonable that at this time the plasma was hot and dense.

The total yield of ablated material, containing both neutral and charged particles, was estimated by measuring the mass of the target before and after the laser irradiation by means of a high-sensitivity digital balance (Sartorius ME215S). The ablation rate was 0.235 μg pulse^{-1}, corresponding to 2.2×10^{15} atom pulse^{-1}. Considering the ion current signal shown in Fig. 5 and taking into account that the relative abundance of Cu^{+2} ions is negligible with respect to that of Cu^{+1} under our experimental conditions [5], the ion yield recorded by the large Faraday cup was 5×10^{13} ion pulse^{-1}, under an acceptance solid angle of 0.12 sr.

4. Conclusion remarks

We have analyzed an expanding Cu plasma produced by an excimer laser of 308 nm, 20 ns and 70 mJ. The laser fluence on the target was about 6 J cm^{-2}. The lowest laser fluence useful for provoking ablation was 0.7 J cm^{-2}. The spot boundary was determined by considering the ablation threshold in the fluence profile. By means of two suitably positioned Faraday cups with a relatively fast signal regime, we observed the suprathermal peak which could be composed of hydrogen ions having an anisotropic energy distribution with an endpoint below 80 eV. The slower peak, corresponding to the Cu ion thermal distribution, had a KL temperature of 5.3×10^5 K and a drift velocity of 5300 m s^{-1}. We also recorded the ejection of electrons from the Faraday cups by the soft X-rays generated from the plasma. We measured an ion yield per pulse of 5×10^{13} particles in the acceptance solid angle of the large Faraday cup, 0.12 sr. The efficiency of our system for particle

https://doi.org/10.1017/S0022377805003910 Published online by Cambridge University Press

production is encouraging in the development of an LIS for ion accelerators or ion implantation.

Acknowledgements

The authors are pleased to acknowledge Mr G. Accoto, Mr P. Esposito, Mr C. Miccoli and Mr V. Nicolardi for their excellent technical support.

References

[1] Luches, A., Martino, M., Nassisi, V., Pecoraro, A. and Perrone, A. 1992 *Nucl. Instrum. Meth.* A **322**, 166.

[2] Woryna, E. et al. 1996 *Appl. Phys. Lett.* **69**, 1547.

[3] Chrisey, D. B. and Hubler, G. K. (eds.) 1994 *Pulsed Laser Deposition of Thin Film*. New York: Wiley.

[4] Miller, J. C. (ed.) 1998 *Laser Ablation and Desorption*. New York: Academic Press.

[5] Torrisi, L., Gammino, S., Andò, L., Nassisi, V., Doria, D. and Pedone, A. 2003 *Appl. Surf. Sci.* **210**, 262.

[6] Miotello, A. and Kelly, R. 1999 *Appl. Surf. Sci.* **138–139**, 44.

[7] Kelly, R. 1990 *J. Chem. Phys.* **92**, 5047.

[8] Qian, F., Craciun, V., Singh, R. K., Dutta, S. D. and Pronko, P. P. 1999 *J. Appl. Phys.* **86**, 2281.

[9] Láska, L. et al. 2000 *Rev. Sci. Instrum.* **71**, 927.

[10] Anisimov, S. I., Bauerle, D. and Luk'yanchuk, B. S. 1993 *Phys. Rev.* B **48**, 12 076.

[11] Miotello, A. and Kelly, R. 1995 *Appl. Phys. Lett.* **67**, 3535.

[12] Kelly, R. and Dreyfus, R. W. 1988 *Surface Sci.* **198**, 263.

[13] Nassisi, V., Pedone, A. and Rainò, A. 2002 *Nucl. Instrum. Meth.* B **188**, 267.

[14] Doria, D., Lorusso, A., Belloni, F. and Nassisi, V. 2004 *Rev. Sci. Instrum.* **75**, 387.

[15] Doria, D., Lorusso, A., Belloni, F. and Nassisi, V. 2004 *Laser Part. Beams* **22** (in press).

[16] Koivusaari, K. L., Levoska, J. and Leppavuori, S. 1999 *J. Appl. Phys.* **85**, 2915.

[17] Nassisi, V. and Pedone, A. 2003 *Rev. Sci. Instrum.* **74**, 68.